Asian Journal of Chemistry; Vol. 23, No. 7 (2011), 3109-3113

ASIAN JOURNAL OF CHEMISTRY

www.asianjournalofchemistry.co.in

# Synthesis, Characterization and Effect of Sintering Temperature on the Humidity Sensing Properties of Nanocrystalline PbO

S.K. KHADEER PASHA, L. JOHN KENNEDY and K. CHIDAMBARAM*

Department of Physics, VIT University, Vellore-632 014, India

*Corresponding author: Fax: +91 416 2243092; Tel: +91 416 2202200; E-mail: kccbb98@yahoo.co.in; khadheerau@yahoo.com

(*Received*: 28 September 2010; *Accepted*: 14 March 2011) AJC-9739

An alcohol thermal route has been used to synthesize nanocrystalline PbO at a relatively low temperature of 75 ºC using lead acetate. The synthesized lead oxide (P75) was subjected to different heat treatments ranging from 200-500 ºC for 2 h to study the effect of crystallinity and phase changes and were further labeled as P200, P300, P400 and P500, respectively. X-Ray diffraction, FT-IR spectroscopy, scanning electron microscopy and transmission electron microscopy were carried out to identify the structural phases, vibrational stretching frequencies, surface morphology and particle size, respectively. The TEM images revealed the change in morphology of PbO from rhombus to rod shape at higher temperatures. The SEM images revealed the porous nature of P75 sample, which is an important criterion for the humidity sensor. All the samples were subjected to dc resistance measurements as a function of relative humidity in the range 5-98 % and the dc resistances at 5 and 98 % relative humidity was used to calculate the sensitivity factor ($S_f = R_{5\%}/R_{98\%}$). Among the different composites prepared, P75 possessed the highest humidity sensitivity of 4545, while the heat treated sample P500 possessed a low sensitivity of 220. The response and recovery time of the maximum sensitivity sample P75 was studied and was found to be 95 and 78 s, respectively.

**Key Words: Nanocrystalline PbO, XRD, Surface morphology, Humidity sensor, Response and recovery.**

## INTRODUCTION

Humidity sensors are needed for humidity control in both residential applications and for industrial processes[1]. Ceramics have been studied extensively as humidity sensors because of their stability in chemical and physical environments[2]. Lead oxide is one of the components of solid state electrochemical cells, ferroelectric, pyroelectric and superconducting oxide materials[3]. In addition, lead oxides are used as gas sensors, lubricants, pigments in paints and also serve as a network former and modifier in oxide glasses[4]. Because of its various applications, considerable progresses have been made on the synthesis of lead(II) mono oxide polymorphs (α-PbO and β-PbO) for many years. Methods such as thermal evaporation[5], sputtering[6], pulsed laser deposition[7], chemical vapour deposition[8], sol-gel, precipitation, solvo-thermal and hydrothermal processes[9] have been adopted for the synthesis of PbO. Recently, the synthesis of PbO nanostructures has gained importance owing to their unusual physico-chemical properties leading to the outstanding applications. Of the available methods, precipitation, hydrothermal and solvo-thermal methods have gained importance due to the fact that they are economically feasible, employ low synthesis temperature and ensure high pure single products. Niasari *et al.*[10], Chen *et al.*[11] and Li *et al.*[12] prepared nanosized PbO and PbO nanocrystals *via* combination of precipitation and thermal decomposition route. Liping *et al.*[13] prepared PbO with one step solid state reaction of Pb(II) compound with NaOH at room temperature, but only α-PbO was obtained by this method. Despite the methods available in the literature for the preparation of PbO and nano PbO, finding an efficient method to produce PbO with size control and orientation by simple methods is still a new challenge to material scientists even today. Hence the present work is focused on the preparation of nanocrystalline PbO by simple precipitation methods at relatively low temperatures. The as synthesized PbO were also treated at different heat treatment temperatures to detect the phase changes and the effect of crystallinity. Though these nano PbO is used for various purposes, the literature regarding usage of PbO for sensing humidity is very scarce. Therefore, the present investigation was focused on the preparation of nano PbO by a alcohol thermal route for the purpose of humidity sensing. The prepared composites were characterized by X-ray diffraction, FT-IR spectroscopy, scanning electron microscopy and transmission electron microscopy. The dependence of electrical response of these compacts towards the relative humidity (RH) was studied. The mechanism of humidity sensing is also suggested.

## EXPERIMENTAL

3.8 g of lead acetate is dissolved in 150 mL of ethanol at room temperature and stirred continuously until a clear transparent solution is obtained. The solution is then adjusted to pH 10 by adding 1N NaOH which results in the formation of a dense precipitate and this is thoroughly stirred using a magnetic stirrer for about 10 h at 75 ºC. This precipitate is then filtered and washed with double distilled water followed by drying in a hot air oven at 75 ºC to yield PbO which is labeled as P75. The as synthesized PbO (P75) is also calcined at different temperatures 200, 300, 400 and 500 ºC for 2 h to study the effect of crystallinity and phase changes and was labeled as P200, P300, P400 and P500, respectively. The calcined powders were subjected to dry milling and made in the form of cylindrical pellets of dimension 13 mm diameter and 3-4 mm thickness using a hydraulic press at a pressure of 400 MPa.

The structural studies were carried out using a Bruker D8 advance X-ray diffractometer for 2θ values ranging from 10-70 ºC using $CuK_\alpha$ radiation at λ = 0.154 nm. A Perkin-Elmer infrared spectrometer was used for the determination of the surface functional groups. The surface morphology of the sintered compacts was determined by a ZEISS scanning electron microscope at the desired magnification. Transmission electron microscope images were recorded using 200 KV HRTEM, model: JEM-2011, Japan to observe the morphology and to determine the particle size of the samples. All the measurements were performed at room temperature.

The dc electrical resistance at different relative humidity levels (RH) of the samples in the form of pellets were determined by a two-probe method instead of the van der Pauw four probe method, as the present work is to measure the changes in surface conductivity as a function of applied field and current. Conducting silver paste was employed to ensure the ohmic contacts. The samples were electrically connected to a dc power supply and a Keithley 614 electrometer in series. Given the high resistivity of the materials under investigation, the potential inaccuracy due to contact resistance is assumed to be negligible. The controlled humidity environments were achieved using anhydrous $P_2O_5$ and saturated aqueous solutions of $CaCl_2{\cdot}6H_2O$, $Ba(NO_3)_2{\cdot}6H_2O$, $Ca(NO_3)_2{\cdot}4H_2O$, $NaNO_2$, $NH_4Cl$, $BaCl_2{\cdot}2H_2O$ and $CuSO_4{\cdot}5H_2O$ in a closed glass vessel at an ambient temperature of 298 K, which yielded approximately 5, 31, 42, 51, 66, 79, 88 and 98 % relative humidity, respectively. Heat cleaning of the samples was found to be a must for the better sensitivity. Hence the sample was heated to 373 K, followed by cooling in a humidity-free atmosphere before and after the sensitivity measurements especially when the sensors were operated at high relative humidity. The samples were exposed to the respective % of relative humidity until the saturation is reached around 1 h. The sensitivity factor, $S_f$ was calculated by using the formula

$$S_f = \frac{R_{5\%}}{R_{98\%}} \quad (\%)$$

where $R_{5\%}$ and $R_{98\%}$ were the dc resistances, at 5 and 98 % relative humidity, respectively.

A degassed glass chamber (200 $cm^3$) was used for the evaluation of response and recovery characteristics. This chamber has a provision for a two-way inlet, one for transpiring dry air from 5 % relative humidity and the other for transpiring moist air from a wet candle containing 98 % relative humidity. The response and recovery characteristics were studied between 5 and 98 % relative humidity conditions. The resistance measurements in dry air as well as in moist air alternatively helped to establish the recovery and response characteristics for moisture sensing.

The temperature dependent conductance experiments for the samples were carried out in the temperature range of 120-300 ºC using a cylindrical furnace attached with microprocessor controlled temperature programmer. The activation energies for electrical conduction of the samples was calculated using the equation:

$$I = I_o \exp^{-E_a/kT} \quad (2)$$

where I is the current, $E_a$, the activation energy, k, the Boltzmann constant and T, the temperature.

## RESULTS AND DISCUSSION

**X-Ray diffraction studies:** Fig. 1(a-e) shows the XRD pattern of the synthesized PbO nanostructures. Fig. 1a is the XRD patteren of P75 sample. All the diffraction peaks can be indexed to monoclinic $Pb_2O_3$ [JCPDS 76-1791], orthorhombic PbO [JCPDS 88-1589] and tetragonal $Pb_3O_4$. The major peaks found for P75 were (100) reflection at 2θ of 12.740º, (110) reflection at 2θ of 14.125º, (200) reflection at 2θ of 20.027º, (202) reflection at 2θ of 24.108º, (211) reflection at 2θ of 26.148º, (111) reflection at 2θ of 29.071º, (200) reflection at 2θ of 30.298º, (020) reflection at 2θ of 32.570º, (210) reflection at 2θ of 34.505º, (310) reflection at 2θ of 34.916º, (212) reflection at 2θ of 35.175º, (400) reflection at 2θ of 40.701º, (112) reflection at 2θ of 44.232º, (220) reflection at 2θ of 45.082º, (300) reflection at 2θ of 46.158º, (421) reflection at 2θ of 47.864º, (402) reflection at 2θ of 49.375º, (511) reflection at 2θ of 54.536º, (222) reflection at 2θ of 60.258º, (410) reflection at 2θ of 65.524º and (023) reflection at 2θ of 68.241º. The same phases were found for P200, P300, P400 and P500 (Fig. 1(a-e)). The patterns were rather complicated, which implied that the material was composed of mixed phases. From the humidity measurements, it is found that P75 showed higher affinity towards moisture.

**FT-IR Spectroscopy:** Fig. 2 shows the FT-IR spectra of all the samples, P75, P200, P300, P400 and P500, respectively. All the spectra exhibit a broad band centered around 3430 $cm^{-1}$ is ascribed to the -OH stretching vibration of water molecule. The appearance of the shoulder around 1630 $cm^{-1}$ is attributed to the H-O-H bending vibrations. These vibrations arise due to the ability of the lead oxides to adsorb moisture from the surroundings during the sample preparation condition for the FT-IR analysis[14]. The shoulder at 1400 $cm^{-1}$ is due to the vibrations of strong bonding of oxygen with Pb. The band at 670 and 438 $cm^{-1}$ is assigned to Pb-O bond vibrations[15].

**Scanning electron microscopy (SEM):** The visual observation of spatial relationships between the component phases in lead oxide is of particular importance in attempts to rationalize their humidity sensing. The surface morphology of P75 and P500 are shown in Fig. 3(a-b). The presence of rhombus shaped crystals with more intergranular pores

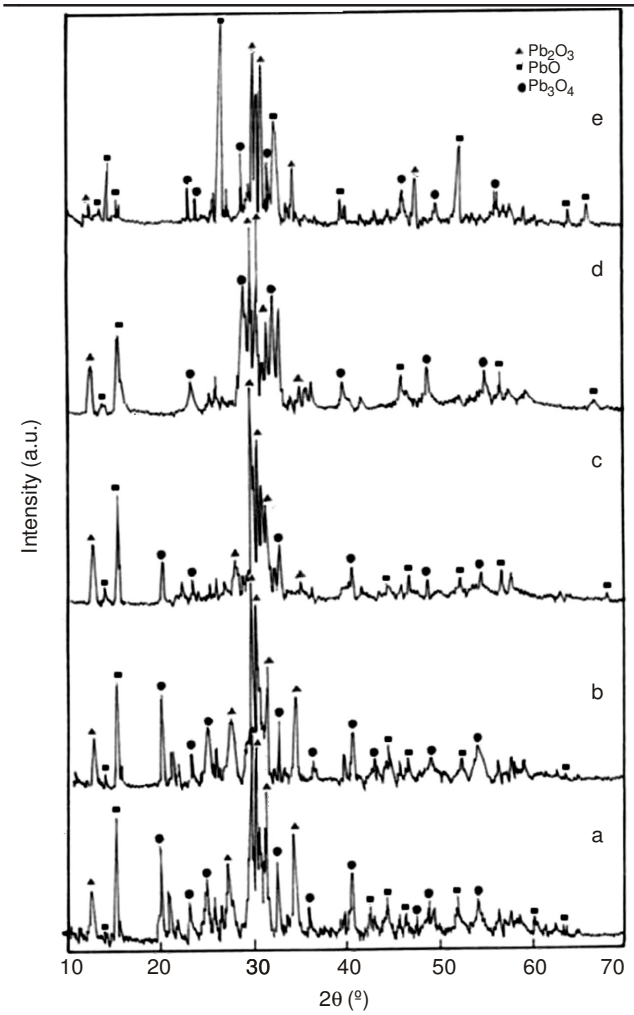


Fig. 1. X-Ray diffraction patterns of (a) P75, (b) P200, (c) P300, (d) P400 and (e) P500

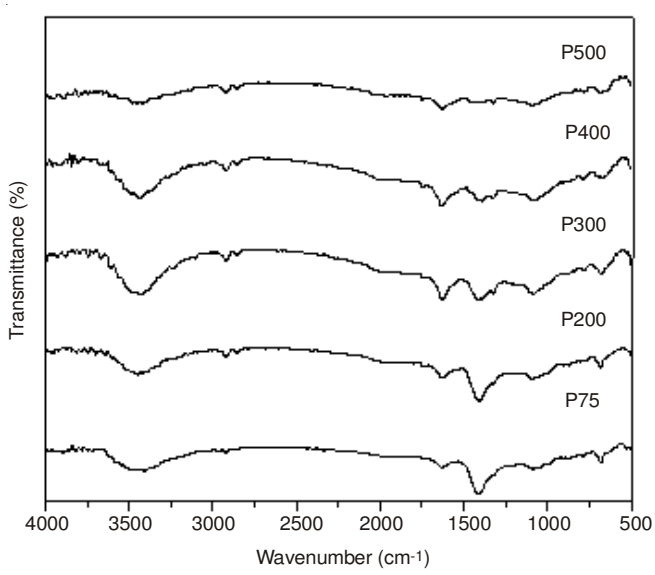


Fig. 2. FT-IR spectra of (a) P75, (b) P200, (c) P300, (d) P400 and (e) P500

confirms the high sensitivity of P75. Although the sample P500 showed the presence of nanorods (Fig. 3b). The presence of lesser porosity proved that this sample is not good towards the sensing of moisture. Thus from SEM studies, it is concluded that the sample P75 is a better sensor towards humidity.

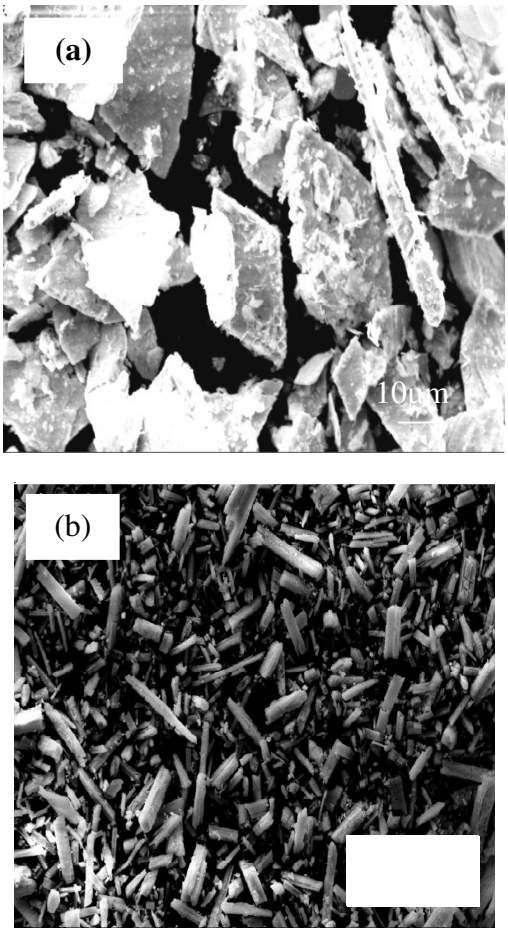


Fig. 3. Scanning electron micrographs images of (a) P75 and (b) P500

**Transmission electron microscopy (TEM):** Transmission electron microscopy image of P75 and P500 samples are shown in Fig. 4(a-b). The image indicates that the sample P75 consists of nanometric particles with diameters of 20-30 nm whereas the sample P500 shows the formation of regular nanorods. The increase in sintering temperature helps only to change the surface morphology from nanoparticles to nanorods. During this change, all the nanoparticles are fused together to grow as a rod and thereby reduce the porosity. However for the sample to be a better candidate for humidity measurements, the presence of porosity is mandatory. By comparing the TEM images, it could be inferred that P75 is a better humidity sensor than P500.

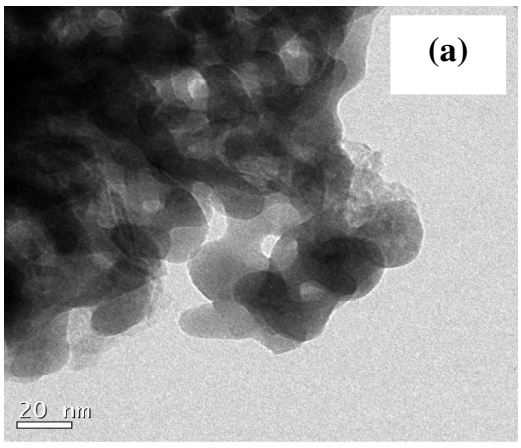

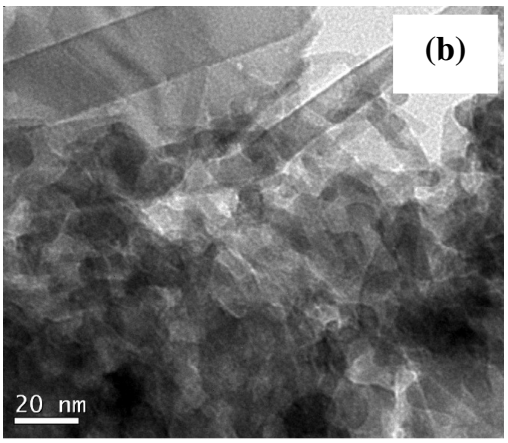


Fig. 4. Transmission electron micrographs images of (a) P75 and (b) P500

**Humidity measurements:** The room temperature electrical conductance measurements of the nano PbO prior to relative humidity measurements signified that the current increased linearly with the applied voltage, indicating the ohmic contact of the electrodes. The temperature dependence of electrical conductance carried out in the temperature range 120-300 ºC suggested that the current (I) increased with an increase in temperature (T). The activation energies calculated from the temperature dependence conductance data are shown in Table-1. The activation energy for electrical conduction in polycrystalline materials generally involves the combination of the energy required to raise the carriers from the dominant levels to their corresponding transport bands and the energy required to create the carriers in the dominant levels. The low activation energy predicts that the small polaron conduction dominates in the studied temperature range[16]. The activation energy increases with increase in the sintering temperature as shown in Table-1. Thus, the higher sensitivity of P75 is confirmed by the presence of lower activation energy. The high activation energy of P500 makes it less prone towards the adsorption of moisture.

TABLE-1
SAMPLE CODE, RESISTIVITY, ACTIVATION ENERGY, SENTIVITY, RESPONSE AND RECOVERY OF THE SAMPLES

| Sample code | Resistivity (Ω cm) | $E_a$ (eV) | $S_f = R_{5\%}/R_{98\%}$ | Response time (s) | Recovery time (s) |
|---|---|---|---|---|---|
| P75 | $2.0 \times 10^{11}$ | 0.3905 | 4545 | 95 | 78 |
| P200 | $1.5 \times 10^{11}$ | 0.7181 | 2640 | 145 | 110 |
| P300 | $1.3 \times 10^{11}$ | 0.7489 | 606 | 179 | 135 |
| P400 | $1.2 \times 10^{11}$ | 0.7616 | 300 | 197 | 158 |
| P500 | $1.0 \times 10^{11}$ | 0.7856 | 220 | 220 | 180 |

The results of resistance measurements as a function of relative humidity (RH) at a fixed ambient temperature of 25 ºC are presented in Fig. 5. The data points on the curve correspond to the average of three measurements made on three samples in order to check the reliability of the results. All the sensor samples studied showed a decrease in resistance values with increase in relative humidity, showing that the conduction occurred mainly at the grain surface, which was governed by the total water molecule content[16]. The resistance changes in the samples with increasing humidity level occur because of adsorption and capillary condensation of water. At low humidity levels, chemisorption takes place, leading to the formation of two surface hydroxyls with the charge transport occurring by the hopping mechanism[17] while at high humidity level, water is physisorbed on the top of the chemisorbed layer.

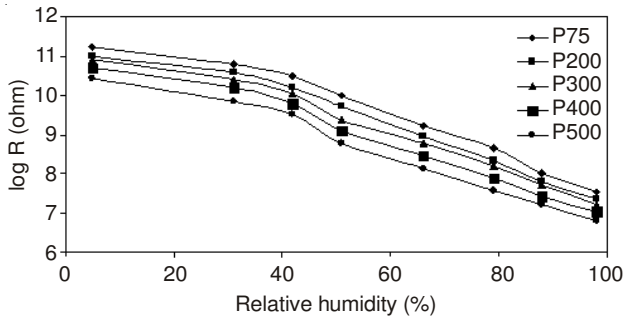


Fig. 5. Relative humidity *versus* log R plots at ambient temperature for PbO

In the present study, it is found that the $S_f$ values, decreases with increase in heat treatment temperature of the samples. Accordingly, the sample P75 possessed relatively high sensitivity value of 4545, while P500 possessed only 220. The occurrence of porosity within the geometry of the PbO nanocrystalline structure in P75 can be accounted for the increase in sensitivity. This induction of porosity increases the total surface area of the PbO gives more space for water vapour absorption. Thus the increase in water vapour adsorption is reflected with the high $S_f$ value of P75. Similarly a very low $S_f$ value of P500 shall be due to the decrease in porosity leading to very less adsorption of water molecules. The SEM and TEM images of P75 supports and signifies the evidence of porosity that could lead to the more sites for water adsorption, which produces more charge carriers for electrical conduction[18]. The observed increase sensitivity of P75 is due to the combination of chemisorption, physorption and/or capillary condensation of water within the pore structure of P75. The $S_f$ values for all the samples shown in Table-1.

The higher sensitivity of P75 can be attributed to the reduced grain size, lower activation energy and the large surface area available for adsorption of water vapour. The fall in resistance is mainly due to the increased amount of conduction electrons or charge carriers upon adsorption of water/gas vapour by the surface layer. Initially the adsorbed water molecules get ionized on the surface and hydronium ions are produced by the assistance of high electric charge density in the neighborhood of the hydroxyl ($OH^-$) sites, resulting in protonic conduction to the adjacent sites. At high humidity the condensation of water in the capillary like pores leads to a liquid like layer leading to electrolytic conduction[18].

**Response and recovery characteristics:** The response and recovery characteristics were studied for all the samples between 5 and 98 % relative humidity for five cycles to ensure the repeatability. The response and recovery time of P75 was 95s, respectively and 75s, where as for P500 it was 220s and 180s,, respectively. This can be explained due to the high sensitivity of P75 and good linearity in the resistance *versus* relative humidity plot. The response and recovery plot of the sample P75 and P500 is shown in Fig. 6(a-b).

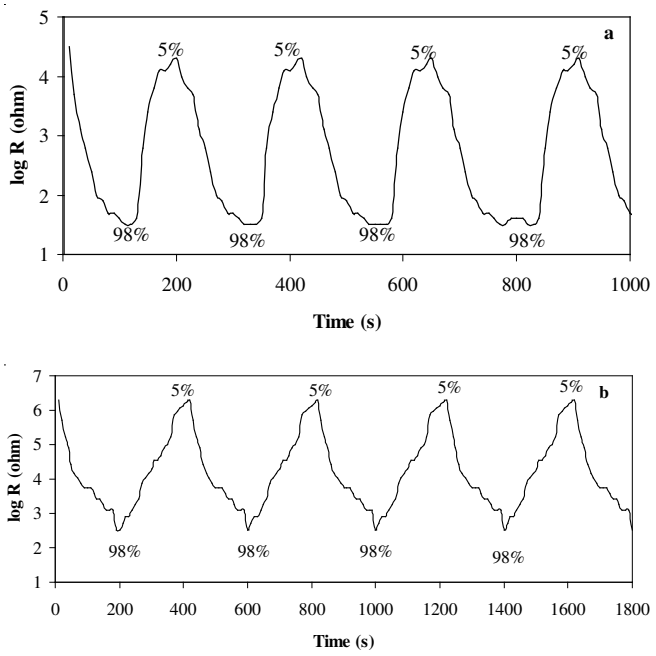


Fig. 6. Response and recovery plot of (a) P75 and (b) P500 composites between 5 and 98 % relative humidity

## Conclusion

Nanocrystalline PbO was prepared by an alcohol thermal route and studied for humidity sensing applications. The results suggest that the sample P75 with more porosity results in high sensitivity value than the corresponding PbO samples sintered at high temperatures (200-500 ºC). The XRD pattern suggested the formation of orthorhomhic $Pb_2O_3$ and with increase in sintering temperature is found that there is an evolution of tetragonal $Pb_3O_4$ phase with simultaneous decrease intensity of $Pb_2O_3$. The vibrational stretching frequencies corresponding to all the samples were confirmed by FT-IR spectroscopy. From SEM and TEM images it is found that the sample P75 consists of nanometric particles with more intergranullar pores where as the sample P500 shows the presence regular nano rods with lesser porosity. Hence the sample P75 is found to be a better candidate for humidity sensing applications as evidenced by the comparatively high sensitivity value. The good response and recovery characteristics of this sample also enable it to be used as good humidity sensor.

## ACKNOWLEDGEMENTS

The authors thank VIT University, Vellore for providing the financial support in carrying out the work.

## REFERENCES

1. W. Wang and A.V. Virkar, *Sens. Actuators B*, **98**, 282 (2004).
2. P. Suman, B. Jeyaraj and K.S. Nagaraja, *Mater. Lett*., **57**, 3543 (2003).
3. A. Wantanabe, T. Tsuchiya and Y. Imai, *Thin Solid Films*, **419**, 76 (2002).
4. G. El-Damrawi and E. Mansour, *Physica B*, **364**, 190 (2005).
5. T.B. Light, J.M. Eldridge, J.W. Mattews and J.H. Greiner, *J. Appl. Phys.*, **46**, 1489 (1975).
6. Y. Pauleau and E. Harry, *J. Vac. Sci. Technol. A*, **14**, 2207 (1996).
7. M. Baleva and V. Tuncheva, *J. Mater. Sci. Lett*., **13**, 3 (1994).
8. L.D. Madsen and L. Weaver, *J. Am. Ceram. Soc*., **81**, 988 (1998).
9. S.Y. Li, W. Yang, M. Chen, J.Z. Gao, J.W. Kang and Y.L. Qi, *Mater. Chem. Phys.*, **90**, 262 (2005).
10. M.S. Niasari, F. Mohandes and F. Davar, *Polyhedron*, **28**, 2263 (2009).
11. L.J. Chen, S.M. Chang, Z.S. Wu, Z.J. Zhang and H.X. Dang, *Mater. Lett*., **59**, 3119 (2005).
12. J. Li, L.Y. Gong and X. Xia, *Yingyonghuaxue*, **18**, 264 (2001).
13. Z. Liping, F. Guo, X. Liu, J. Cui and Y. Qian, *J. Cryst. Growth*, **280**, 575 (2005).
14. V. Timar, R.L. Ciceo and I. Ardelean, *Quant. Elect. Optoelect.*, **11**, 221 (2008).
15. S. Li, W. Yang, M. Chen, J. Gao, J. Kang and Y. Qi, *Mater. Chem. Phys.*, **90**, 262 (2005).
16. Z.A. Ansari, T.G. Ko and J.H. Oh, *Surf. Coat. Technol*., **179**, 182 (2004).
17. J.J. Vijaya, L.J. Kennedy, G. Sekaran and K.S. Nagaraja, *Sens. Actuators B*, **124**, 542 (2007).
18. J.J. Vijaya, L.J. Kennedy, G. Sekaran and K.S. Nagaraja, *Sens. Actuators B*, **127**, 619 (2007).